Physics Utrecht
EMMEΦ

Utrecht University

Institute for Marine and Atmospheric Research Utrecht

Bachelor thesis

# The relative contribution of snow and ice melt on runoff

*Author:*
Thom Wolf

*Supervisor:*
Dr. Willem Jan van de Berg

June 15, 2016

**Abstract**

The Greenland ice sheet (GrIS) has shown an increase in total runoff in the decades since 1950. This bachelor thesis investigates the relative contribution of snow and ice melt to the increase in runoff of the Greenland ice-sheet over the past 57 years since 1958. Also the change of buffering effect that refreezing has on the runoff in this period is investigated. This is done by using data from the regional atmospheric climate model: RACMO2.3.

The available RACMO2.3 model data has been analyzed by dividing the GrIS into 4 sub-areas with different melt characteristics. The 4 sub-areas are respectively characterized by a high runoff from ice (1), high runoff from firn (2), refreezing (3) or no significant melt(4). The data showed that there has been an increase in ice runoff, firn runoff and refreeze over the past 50 years in the GrIS. Especially since 1990 these increases are very strong. The runoff from ice has increased in all the four areas. The runoff from firn only increases in areas 2,3 and 4. The refreezing only increases in areas 3 and 4. The data showed that the runoff from ice has increased more than the runoff from firn in the last 57 years and is leading to a larger contribution to the reduction of the surface mass balance ($SMB$) than the runoff from firn. Since the ice runoff is primarily ice melt, and the firn runoff primarily firn melt, we can conclude that the ice melt is the biggest contributor to the reduction of the $SMB$. Having investigated the components of the surface energy balance we found that the short wave net energy flux has increased in the past decades and correlates very good with the total melt. The ground heat flux decreases at places where the refreeze decreases and therefore decreases at places where the ice runoff grows. The latent heat flux shows in areas 1 and 2 an increase and shows a good positive correlation with the windspeed at 10 meter elevation. In areas 3 and 4 the latent heat flux shows a decrease and has here a good negative correlation with the temperature at 2 meter elevation.

# Contents

# 1 Introduction

The Greenland Ice sheet (GrIS) is the second largest ice sheet in the world covering around 80 percent of the total area of Greenland. Since the beginning of the centrury it has shown an increase in mass loss. Research has showed that between 1992 and 2011 the ice sheets of Greenland, East Antarctica, West Antarctica, and the Antarctic Peninsula changed in mass by $-142 \pm 49$, $-14 \pm 43$, $65 \pm 26$, and $-20 \pm 14$ gigatonnes per year, respectively [1]. This shows that the GrIS has lost more mass than the other icesheets. The increased pace of losing mass is for the GrIS higher than in the Antartics [2]. Due to the global warming, the GrIS undergoes an enhanced surface melt. The GrIS contributes at the moment to around 70% of the total melt that the GrIS, the Antarctic Peninsula and parts of West Antarctica are losing together[2]. If all the ice on Greenland were to melt, the sea level would rise approximately 7.3 m [3]. Because of the many consequences of such a sea level rise, the mass balance of the GrIS is being investigated in detail. Climate models are being developed to get insight in the past, present-day and future climate systems in the polar regions.

## 1.1 Climate and geography of Greenland

Greenland is located between between latitudes 59 and 83N, and longitudes 11 and 74W. It is the largest non-continental island of the world and has the second largest ice sheet. Around 80 percent of the total area is covered with ice and snow. The GrIS contains around 7 percent of the total fresh water volume in the world. Greenland is surrounded by the Artic Ocean in the north, the Greenland Sea in the east, the Atlantic ocean in the southeast and the Baffin Bay in the west. The GrIS can reach elevations of around 3000m. The highest elevations are reached along the coastal line from the south-east towards the north-east. The regions along the coastal lines, especially in the south of Greenland have a milder climate. Temperatures rise here often above 0 °C, while on the interior of the icecap temperatures can drop below -50 °C in the winter. The south-east of Greenland is wetter than other regions of the island. The interior and the northern part of the ice sheet are the driest.

## 1.2 Research question

The Greenland ice sheet (GrIS) has shown an increase in melt water runoff since 1958. This increase has also been modeled by the regional climate model RAMCO2.3. The increase in surface temperature during this period is known to be the most important cause of the increase in melt water runoff. So far it is unknown to what extend snow melt and ice melt have each contributed to the increase in melt water runoff. This will be investigated in this thesis. In order to explain the differences between melt and runoff, refreezing must be analyzed too. After the investigation of these processes, we will also look at possible drivers for the increase in melt and runoff. The changes in components of the surface energy balance are compared with the changes of the melt and of other subsurface processes.

# 2 Data and Model description

## 2.1 General model description

For this bachelor theses we have used the data output of the Regional Atmospheric Climate Model (RACMO), version 2.3. The dynamic core has been taken from the regional climate model HIRLAM (version 5.0.6) and the physics from the integrated forecast system (IFS) of the European Center for Medium range Weather Forecasts (ECMWF), version CY33R1. The dynamics describes the evolution of the large scale flow and transport of heat and moisture. The physics describes the effect of subscale flow due to turbulence and convection, clouds, surface-atmosphere interactions and radiative transport. [4] It was originally developed for present-day and future climate integrations over Europe [5]. RACMO2.3 is now often used to describe the climate of arctic regions like Greenland. Additional to the existing atmosphere-surface interaction, RACMO2 has therefore been extended with a detailed module that describe the atmosphere-ice sheet interaction and the subsurface processes on large glaciers and ice sheets. The subsurface processes included are melt water percolation, retention, refreezing and runoff, snow compaction and grain size evolution that effects the surface albedo of the snow or ice surface. The model needs external information at the lateral boundaries and sea surface. For this study the interior of the domain is allowed to evolve freely [5] and is not forced at the top. The model is forced by a global atmospheric reanalysis ERA-Interim every 6 hours at the lateral boundary zone with the temperature, specific humidity, zonal and meridional wind components, the surface pressure, the sea surface temperature and sea ice concentration. The simulation starts in September 1957 and almost all the data is available for all the years up to 2015. The data of the surface energy balance components is only available up to 2014. The RACMO2.3 model output data that we use for the GrIS has $312 * 306$ gridpoints defined on a rotated spherical grid, with an average resolution of $11 * 11$ km. The model domain includes Greenland, Iceland, Svalbard, the northern part of Canada and the oceans around these islands. The model consists of 40 vertical layers with the lowest layer at 10 meter. The raw model output exists of 3, 6 and 24 hourly instantaneous and accumulated data, which is processed into daily, monthly and yearly averages and sums. For analyzing the model data we use the NCL (NCAR command language) language package. Because only the results for domain of the GrIS are required, a mask has been used to filter out the unnecessary results. To get integrated data, the data is summed over the area. Here is an correction function applied to get the exact gridsize at each latitude and longitude.

## 2.2 Snow model and energy balance

The surface mass balance ($SMB$) and surface water balance ($SWB$), as modelled by RACMO2.3, consist of the following components:

$$SMB = Snowfall + Rainfall - SU - RU \tag{1}$$

$$SWB = Melt + Rainfall - Refreeze - Runoff \tag{2}$$

In which Su is the surface sublimation and RU is the runoff.
The runoff RU is defined as:

$$RU = Melt + Rainfall - Refreeze - Retention \tag{3}$$

For this research is the retention assumed to be very small and is therefore neglected. We divided the runoff into runoff from ice and runoff from firn. Runoff from ice occurs on areas with ice at the surface. This is usually called the surface runoff. The surface runoff is the drainage of water on top of a surface of ice. Runoff from firn occurs on areas with a firnlayer at the surface. This is usually called the deep runoff. The deep runoff is the drainage of water that has percolated through a firnlayer and eventually reached the ice beneath the firnlayer. In this research we will only use the terms ice runoff (= runoff from ice) and firn runoff (= runoff from firn). The melt, rainfall and refreeze can also be divided into a part that comes from areas with ice and with a firnlayer at the surface

The initial data files and assumptions are not fully used in this research, because RAMCO2.3 calculates that during rainfall, there will be a small amount of snowfall. This forms together a thin layer of a snow water mixture. Due to this thin mixture, RAMCO2.3 assumes that there will be only runoff from firn and no runoff from ice at those places when there is rainfall. The initial output ice runoff is therefore less than what could be regarded as ice runoff without significant snow or firn cover. Therefore we created for this thesis new output data with the assumption that there can only be firn runoff if a site has at the beginning of the day a firn layer with more than 2 cm of pore space. If the firn layer is thinner or absent at the start of the day, any runoff for that day is regarded as ice runoff. Using the same criteria, melt, refreezing and rain has been split out to melt of, refreezing in and rain on ice and firn.
Originally the refreeze was defined to interfere only with the firn melt and therefore with the runoff from firn. With our new assumption refreezing can also occur in the 2cm layer and interfere with the ice melt and therefore with the ice runoff. This ice refreezing is however expected to be negligible.
We now use the new created data: runoff from ice (surface runoff), runoff from firn (deep runoff), melt of ice, melt of firn, refreeze in ice, refreeze in firn, precipitation on ice and precipitation on firn. We will not investigate the sublimation, due to its small contribution to the $SMB$ and because it has not shown a significant change in the last decades.

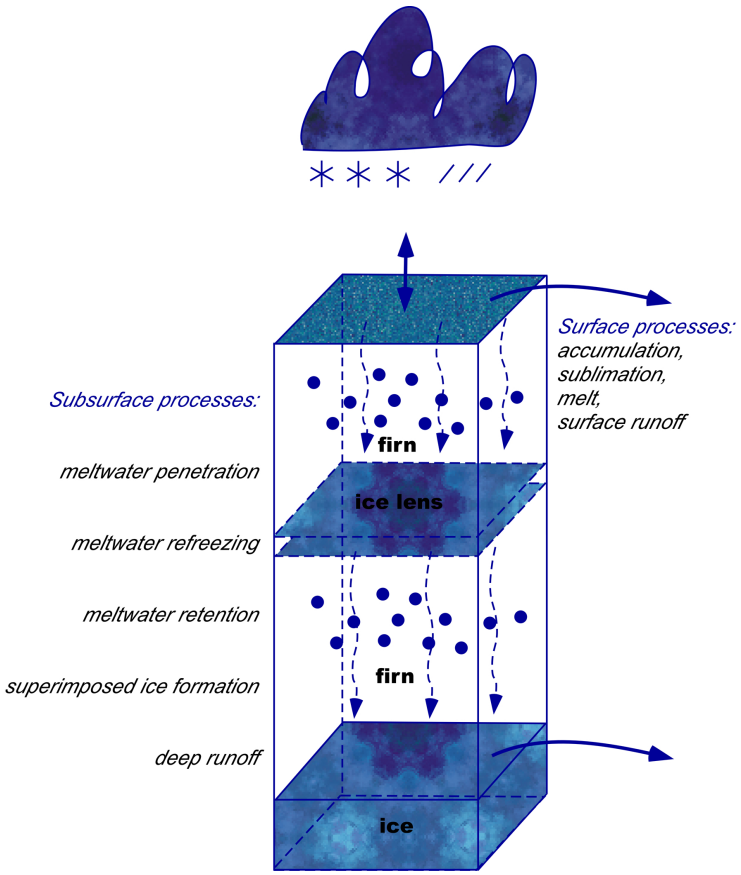


Figure 1: Schematic representation of the modelled processes that determine the surface mass balance ($SMB$) [5]

The surface energy balance ($SEB$) is defined as:

$$\begin{aligned} M &= SW_{net} + LW_{net} + SHF + LHF + GHF \\ &= SW_{down} + SW_{up} + LW_{down} + LW_{up} + SHF + LHF + GHF \end{aligned} \tag{4}$$

In which $M$ is the total melt energy, $SW$ is the short wave radiation, $LW$ is the long wave radiation, $SHF$ the sensible heat flux, $LH$F the latent heat flux and $GHF$ the ground heat flux. Here, the energy balance components are positive if they are pointed towards the Earth's surface.
The $SW_{down}$ is the downwelling short wave radiation from the sun. A part of this radiation is directly reflected, depending on the surface albedo. The incoming short wave radiation minus the reflected short wave radiation gives the $SW_{net}$. The $LW_{up}$ is the outgoing long wave radiation emitted by the Earth. $LW_{down}$ is the long wave radiation coming towards the surface mainly emitted by the clouds and the atmosphere. The $SHF$ and $LHF$ are the sensible and latent heat fluxes, respectively, which are often called as the turbulent fluxes. The $SHF$ represents the transfer of energy due to the difference in temperature between the surface and the atmosphere. It is mostly influenced by temperature gradients and turbulence in the air created by strong (katabatic) winds. The $LHF$ is the flux of energy that is needed or released

if water evaporates from or sublimates on the surface, respectively [6]. The $LHF$ is thus strongly connected to the humidity as well as to the temperature, as warm air can contain more moisture than cold air and ice sheet surface temperatures are bound to 0 °C. Figure 2 shows the processes in the boundary layer that have an influence on the ice sheet.

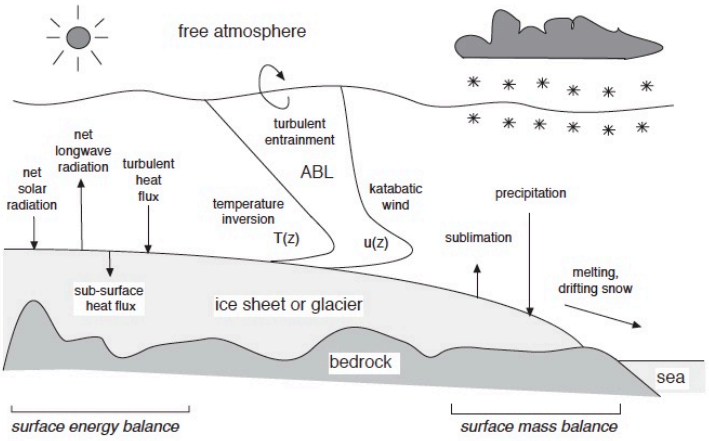


Figure 2: Processes of the atmospheric boundary layer over an ice sheet [7]

# 3 Results

## 3.1 Firn and ice melt

### 3.1.1 Integrated data

Figure 3 shows the yearly integrated values of components of the $SWB$ for the total GrIS. Equation 2 for the $SWB$ shows that melt and rainfall are the sources and the refreeze and runoff the sinks. Following Figure 3, the biggest source is the firn melt followed by the ice melt. The melt of firn and ice has a much larger contribution to the $SWB$ than the rain on ice and rain on firn. The biggest sinks are the ice runoff and the refreeze in firn. They are followed by the firn runoff. The refreeze in ice is very small, as we assumed. The values of all the components do not form smooth lines, but give lines with an interannual variability. Further, it shows that the runoff from ice is larger than the runoff from firn and increases faster than the runoff from firn and the refreeze in firn. It will therefore contribute more to the total runoff than the firn runoff does. The ice melt follows exactly the trend of the runoff from ice. This is due to the little refreeze in ice and little rain on ice. The total firn melt is higher than the total ice melt but the ice melt increases faster. Comparing the firn runoff with the firn melt shows that the latter has higher values and increases more. This is due to the high values of the refreezing in firn, which also shows an increase. The ice melt and the ice runoff are approximately equal and show thus both the same largest trend of all the $SWB$ components.

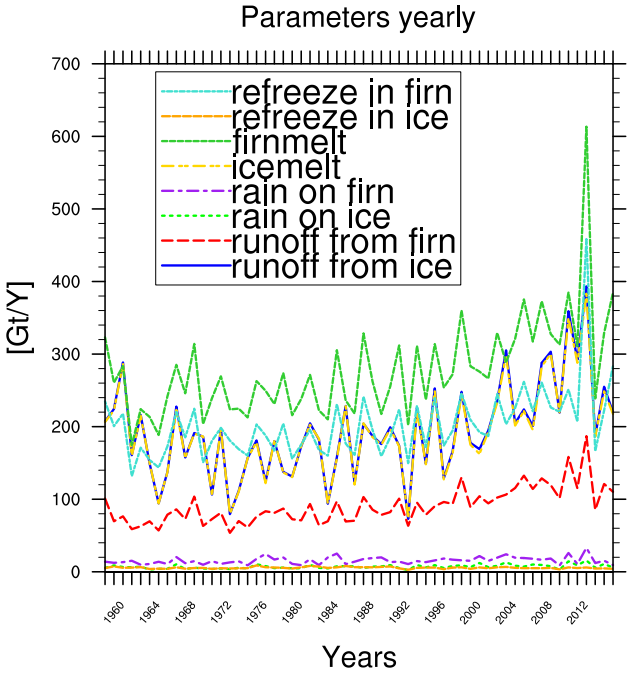


Figure 3: Total plot of yearly values of $SWB$ components integrated over the total GrIS.

### 3.1.2 Areas

To get a better understanding of the increase in the ice and firn melt, we divided the GrIS into four areas (Figure 4). We defined these four areas by considering the runoff from ice and firn and the refreezing at each gridpoint and looking which has the highest value at that gridpoint, using 1957-2015 averages. In area 1 is ice runoff the largest. In area 2 is firn runoff the largest. In area 3 is the refreeze the largest. Area 4 experiences no significant melt. Assumed is here that melt is not significant if it is lower than 30 $kg/m^2$. Area 1 is mostly concentrated in the south-east and north-west of Greenland. Area 2 is mostly concentrated in the south-west of Greenland. Areas 3 and 4 lie in the interior of the ice-sheet from north to south. Figure 4 shows that the ice and firn runoff occur mostly in the ablation zones at the edges of the GrIS. By looking at time series of several arbitrary chosen gridpoints for each area on the GrIS, we could see that these areas have different climates. Areas 1 and 2 are warmer than areas 3 and 4. Area 2 is a region with much precipitation compared to the other three areas. Dividing the ice-sheet in four different areas, shows the trends and interactions between the runoff, refreezing, ice and firn melt and precipitation. These four areas have been used as masks in the original data to get the data per area.

By using these four regions, we can make timeseries for each region. Because the regions have a different area, we use the averaged values of each area instead of the summed values (Figure 5). This gives a better insight in the melting process for each area.

In Figure 5(a) of area 1, we can clearly see that the ice runoff is the largest $SWB$ component in this area and increases the most. The refreeze and firn runoff are decreasing. The firn runoff and the snowfall are approximately equal. The data shows that almost all the snowfall in area 1 occurs in the winter. Therefore, the firn runoff in this area comes for a large part from the melt of the firn that is created by snowfall in the winter (not shown). After this firnlayer has undergone refreeze in firn, firn melt and firn runoff during the melt season, there will be mainly ice runoff. The ice melt is following the trend of the ice runoff because there is no significant change in the refreeze in ice and the rain on ice. The firn melt is decreasing in the same way as the firn runoff and the refreezing are decreasing.
Figure 5(b) of area 2 shows that the firn runoff is bigger than the ice runoff and the refreeze. The firn melt is here bigger than the ice melt. The snowfall in this area is very heavy, but shows a decrease. The snowfall is here larger than the firn melt. In this area the refreeze is decreasing too, which gives rise to a stronger increase in the firn runoff than the firn melt. Although the ice melt is low, it shows a strong increase, followed by an equal increase in the ice runoff. There is significantly more rainfall on firn in area 2 than there is rainfall on firn and on ice in area 1, as we already knew by defining this area.
Figure 5(c) of area 3 shows that the refreeze in firn is larger than the ice and firn runoff. The firn melt is higher than the refreeze. In the first years, the firn melt and refreeze seem to increase parallel to each other, but deviate from each other at later years. So the fraction of firn runoff from the firn melt is increasing over time.

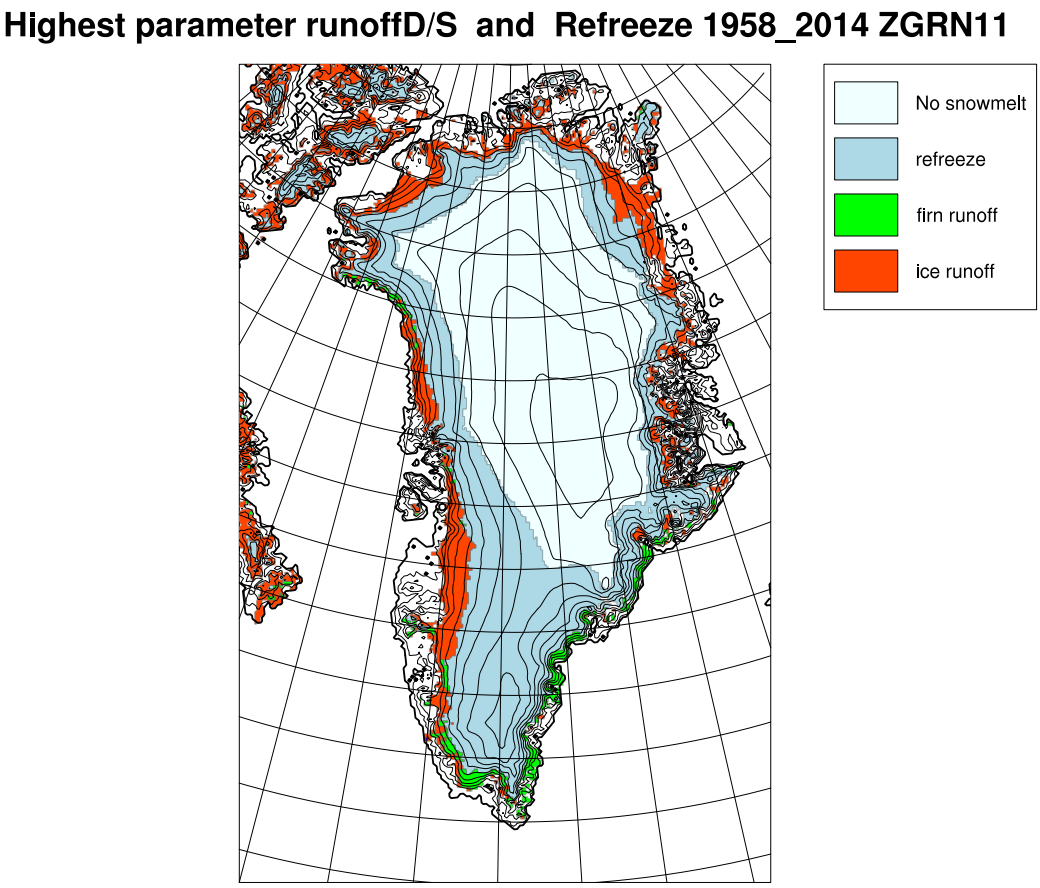


Figure 4: Plot of the GrIS showing the four defined areas. Area1: ice runoff highest (red), Area2: firn runoff highest (green), Area3: refreeze highest (blue), Area4: No significant melt ($< 30kg/m^2$) (grey).

Although the values are low, the ice melt and ice runoff also show an increase.
Figure 5(d) of area 4 shows that the total runoff is almost zero. The only significant components are the refreezing in firn and the firn melt. The firn melt doesn't provide a high firn runoff because literally all the water will refreeze. Although the ice and firn runoff are very low in this area, they still show an increase.
Comparing the $SWB$ components of these subfigures of figure 5, the data shows that the ice runoff increases in all four areas. The firn runoff increases in areas 2 up to 4 and shows a decrease in area 1. The refreeze increases in areas 3 and 4 and decreases in areas 1 and 2.

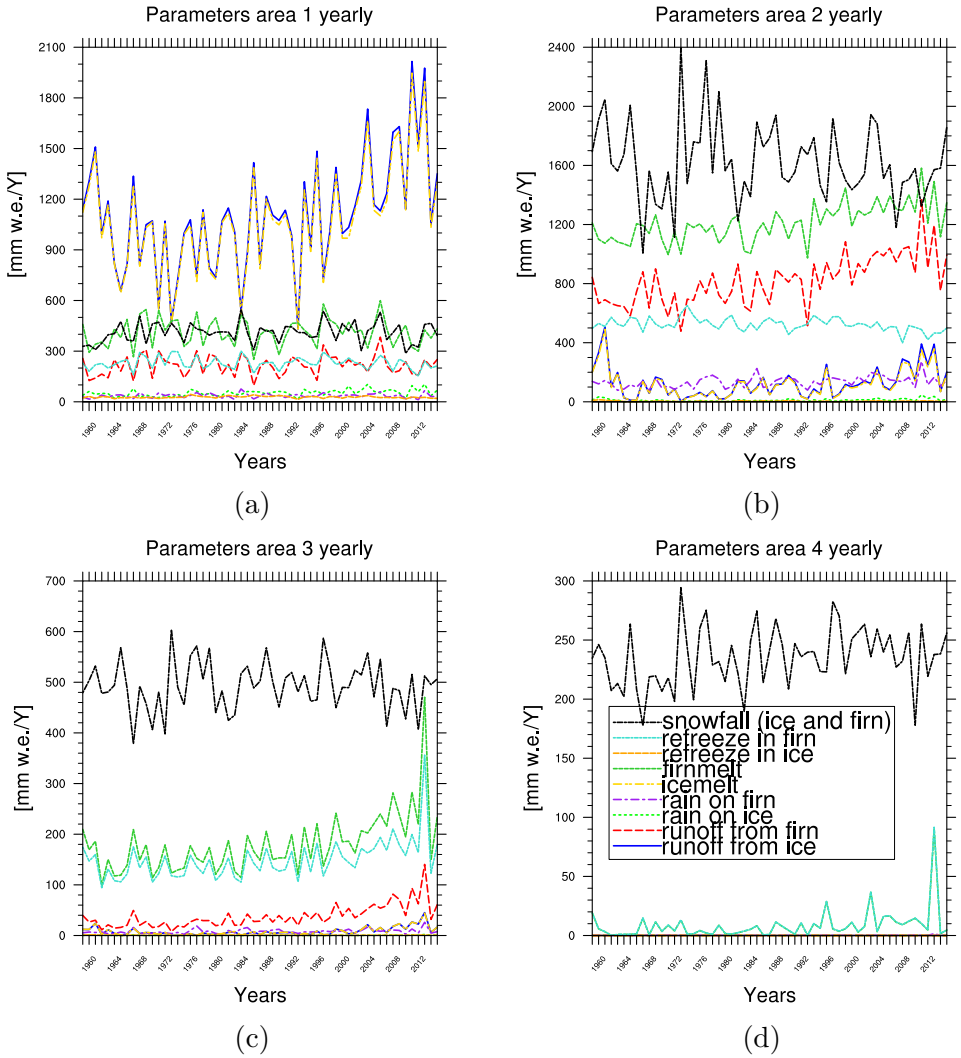


Figure 5: Timeseries of yearly values of $SWB$ components per area averaged over each area

### 3.1.3 July/Summer data

The winter has approximately no melt and is thus not of interest for investigating the melt. A change in melt can therefore better been investigated if we look to the summer months. The subfigures in Figure 6 show the $SWB$ components for the summer months averaged over all 57 years. The figures clearly show that the runoff and either refreeze or melt have their maximum in the month July. It also shows that the snowfall is low in the summer months compared with the yearly values of snowfall in Figure 5. Subfigure 6a gives a good indication of how the melting process evolves in the ice ablation region (area 1). It shows that the firn melt has a maximum in June and decreases to zero in July and August. In July there is a peak in melt of ice and a peak in the ice runoff. This indicates that at the beginning of the summer, there is still some snow on top of the ice. As the summer continues, more ice comes to the surface and the melt of firn and the refreeze in firn will decrease and

the melt of ice increases. Subfigure 6b shows that in area 2 the firn melt is higher than the refreeze. In the early summer the firnlayer is cold. When the firn melt begins, the refreeze in firn begins also. The refreeze increases and heat is released in the firnlayer due to this refreezing. As the melt season continues the firnlayer will become warmer. In July comes the point that a large part of the firnlayer is fully warmed up to 273K. Therefore the refreezing in the firnlayer will drop. Due to this drop in refreezing, the firn runoff will grow. Subfigure 6c shows that the firn melt in area 3 is much lower than the firn melt in area 2. The refreeze in firn is here larger than the firn runoff. The firnlayer will only partially warm up to 273K in July and therefore the refreeze won't show a decrease, but will only show a less steep increase. The runoff from firn will still grow, but not as fast as in area 2. Subfigure 6d shows that the firn melt and the refreeze of firn are approximately equal and that there is almost no firn runoff.

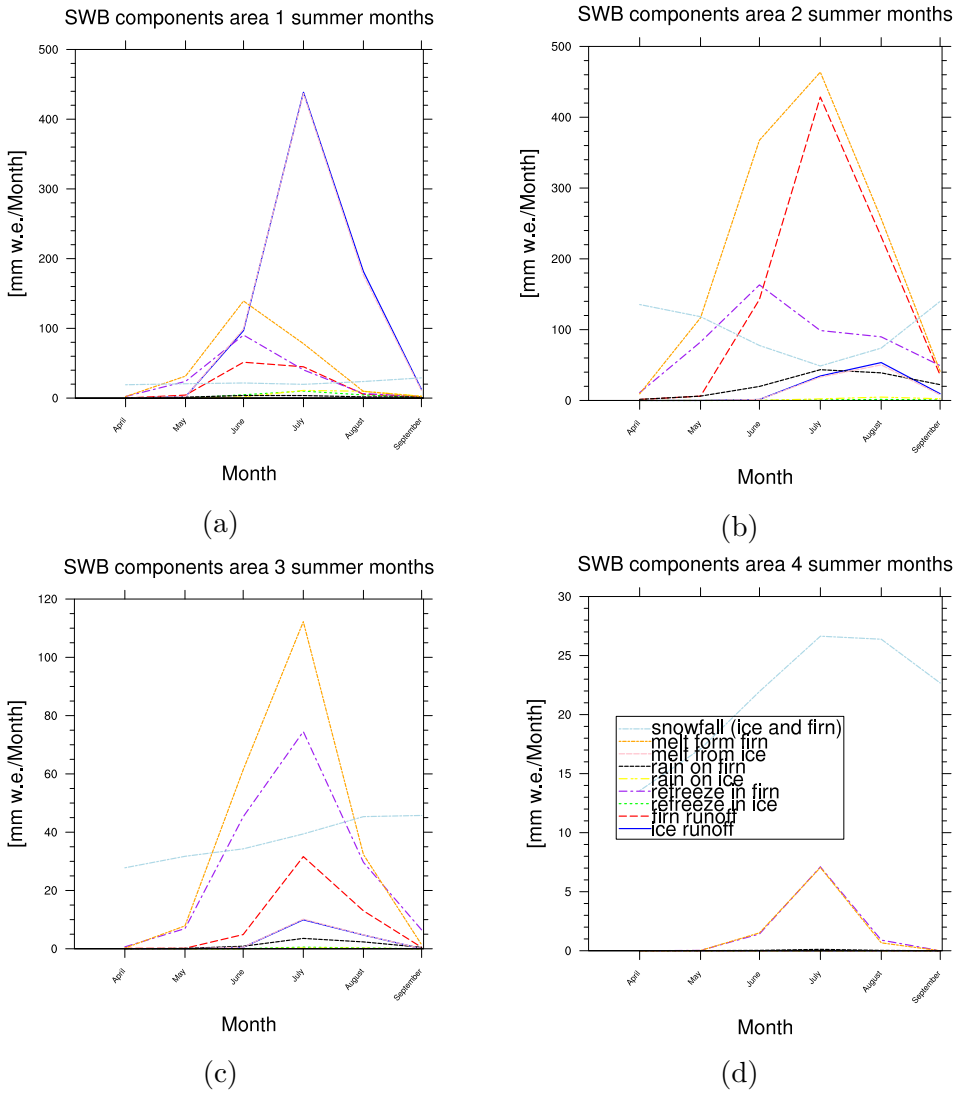


(a) (b) (c) (d)

Figure 6: Summer months values per area of the $SWB$ components averaged over all 57 years

The data shows that the summer months are the only months with significant melt, with a large peak in July. The other months have approximately no melt. We will therefore look mostly to the $SWB$ components in July. Figure 7 shows the timeseries of the ice and firn runoff in July over the last 57 years. The values are averaged over each area. It shows that the ice runoff increases in all areas and that the firn runoff increases in areas 2, 3 and 4 and decreases in area 1. The slope of the linear approximation is higher for the ice runoff in area 1 than the slope of the firn runoff in area 2. Figures 8 shows that there is a higher increase in ice melt in area 1 than the increase in firn melt in area 2, which can cause this stronger increase in ice melt in area 1 than firn melt in area 2. Figures 7 and 8 show together, that the linear line approximation of the firnmelt in area 2 has a lower slope of increase than the firn runoff in area 2. This can be explained by the strong decrease in refreeze of firn in area 2 (Figure 9). Figure 9 also shows that the averaged values of the area for the refreeze in firn are a tenfold higher than those of the refreeze in ice. The refreeze in ice shows a decrease in area 1 and an increase in areas 2, 3 and 4. The refreeze in firn shows a strong decrease in areas 1 and 2 and an increase in areas 3 and 4. The firn melt in Figure 8 shows a decrease in area 1. This can be due to either less snowfall in the winter, or to a shift of the melt seasons towards June, so that there is less firn to melt in Juli. The data showed that the snowfall hasn't changed in area 1 in the last 57 years. Therefore we compare the firnmelt in June with July to investigate the possible shifting of the melt season. Figure 10 suggests that the melting season is changing in area 1 since 1990. The melting of firn in area 1 in July decreases, while it increases in June. For area 2 is the increase in June higher than in July which also suggests the shifting of the melt season this area.

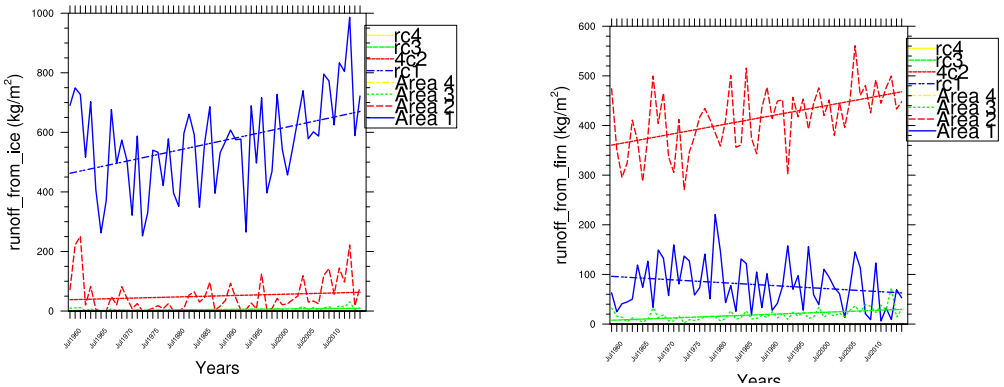


(a) (b)

Figure 7: Timeseries of ice runoff (a) and firn runoff (b) in July

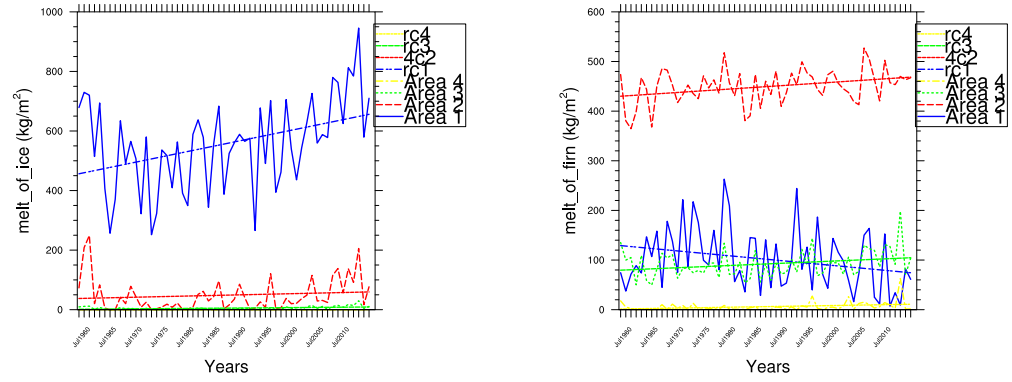


(a) (b)

Figure 8: Timeseries of ice melt (a) and firn melt (b) in July

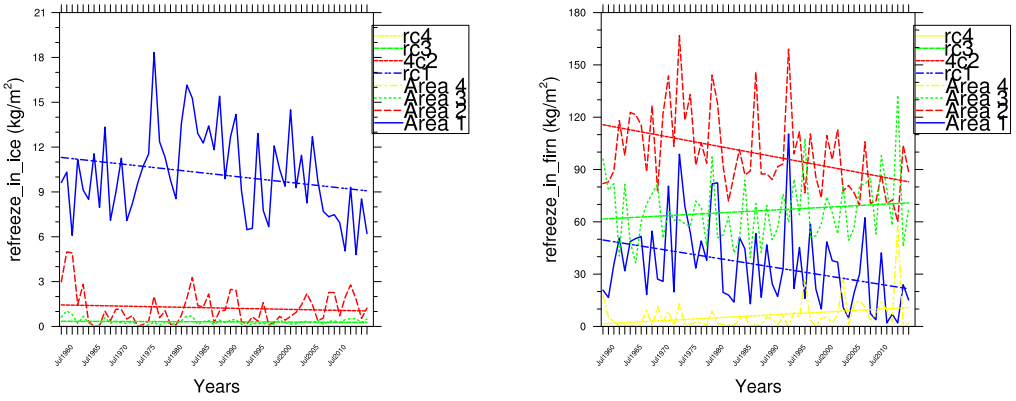


(a) (b)

Figure 9: Timeseries of refreeze in ice (a) and refreeze in firn (b) in July

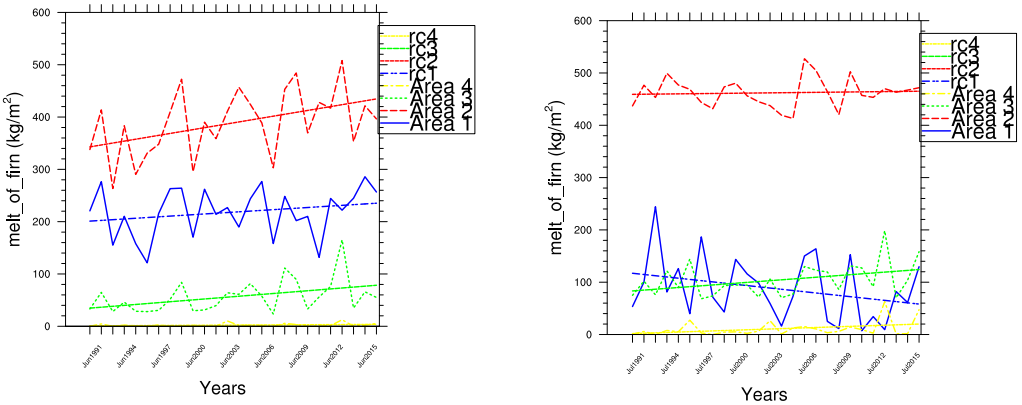


(a) (b)

Figure 10: Timeseries of melt of firn in June (a) and July (b) since 1990

The linear correlation plots of the runoff, refreeze, melt of ice and melt of firn with the total melt for the month July for the whole GrIS (not included in this paper), show that the ice runoff and firn runoff have approximately the same correlation with the total melt. It does however not show the processes behind these correlations. It is therefore better to look at the correlation plots for the four separate areas. Figure 11 shows that integrated values of the ice runoff have a very good correlation in area 1 ($R = 0.94$) and in area 2 ($R = 0.75$) with the total melt. The runoff from firn shows in area 1 a weak negative correlation ($R = -0.34$). In area 2, the firn runoff has a weak positive correlation ($R = 0.53$). These correlation plots show that the total melt in area 1 correlates better with the ice runoff than with the firn runoff. Figure 7 already showed that the ice runoff increased and firn runoff decreased in area 1. Which confirms the better correlation of the ice runoff with the total melt in area 1. Despite the fact that the firn runoff is larger and increases faster than the ice runoff in area 2, the correlation plots show that the ice runoff correlates better with the total melt in area 2 than the firn runoff does. This is due to the small increase in melt of firn, which accounts for most of the melt in this area (Figure 8). The increase in ice runoff here is less than the increase in firn runoff and therefore, the ice runoff will correlate better with the total melt.

Figure 12 shows the correlation of refreezing in firn with the total melt per area. It shows that the refreeze in firn has a negative correlation in areas 1 with $R = -0.54$. Here the mass (Gt) of the total melt is a 10 fold higher than the total mass of the refreeze. In area 2 the refreeze in firn has a negative correlation with $R = -0.53$. In this area is the value of the refreeze in firn closer to the total melt. The refreeze in firn and the total melt correlate perfect in are 3 with $R = 0.97$ and in area 4 with $R = 0.99$. The total mass of the refreeze in firn is here approximately equal to the mass of the total melt, which indicates that refreeze is the most dominant sink of the $SWB$ in areas 3 and 4. The figure also shows a decrease in refreeze in firn in areas 1 and 2 and an increase in areas 3 and 4. This means for area 1 that the decrease in firn runoff will be less than the decrease in firn melt.

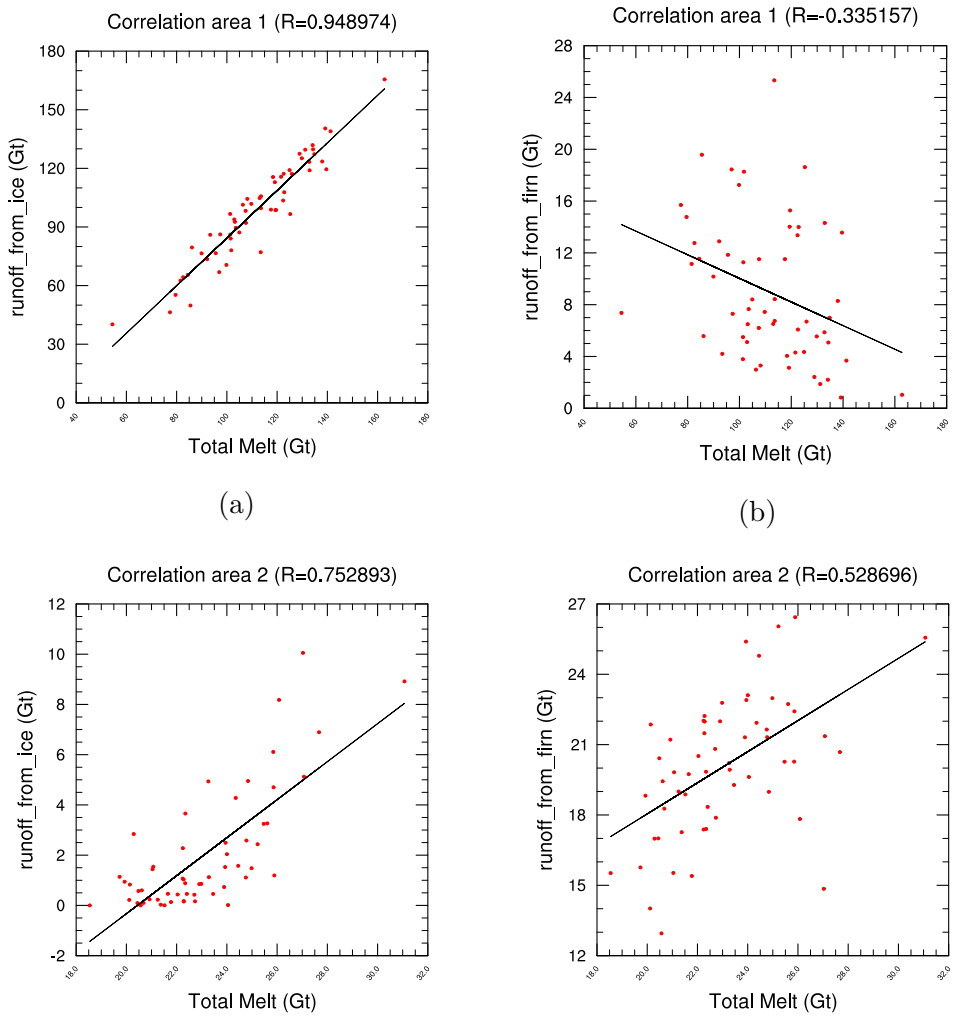


Figure 11: Correlation in July between ice/firn runoff (a,c and b,d respectively) and the total melt for area 1 (a,b) and 2 (c,d)

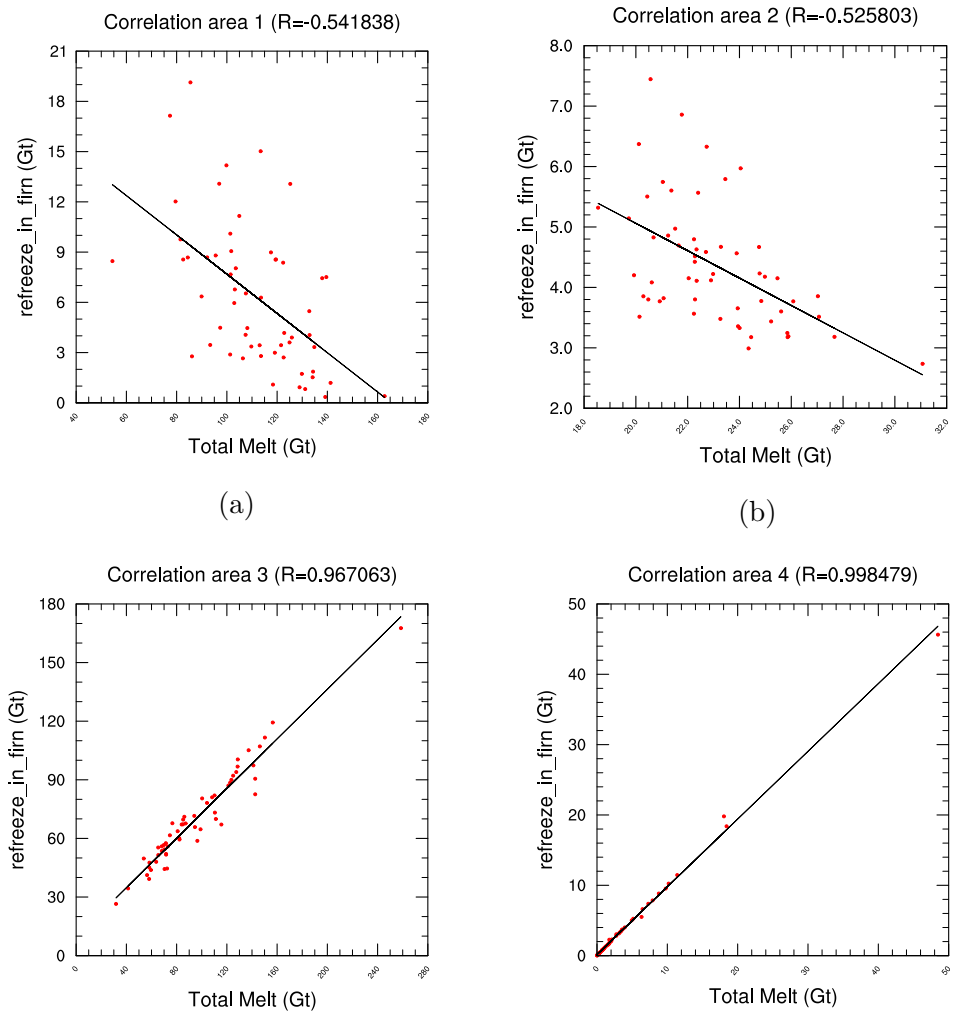


Figure 12: Correlation in July between refreezing in firn and the total melt for (a) area 1, (b) area 2, (c) area 3 and (d) area 4

## 3.2 Energy balance

Not only understanding, but also finding driving mechanisms of the increase in runoff and melt is important. Therefore we look at the components of the $SEB$ averaged over all 56 years since 1958 (Figure 13a). It shows that the net $SW_{net}$ has a maximum in July in all areas. This is especially the case in area 1 and is the highest of the four areas. The $SW_{down}$ has in all areas a maximum in June. The data shows that area 1 and 2 have less $SW_{down}$ than areas 3 and 4 (not shown). The fact that the $SW_{net}$ is the highest in area 1, has to do with the albedo effect. In Figure 13b the cloudcover and albedo are plotted. It shows that the albedo decreases as the summer continues, with a minimum in July. Especially area 1 has a very low minimum. Due to this low albedo more short wave energy will be absorbed and the snow/ice will warm up.

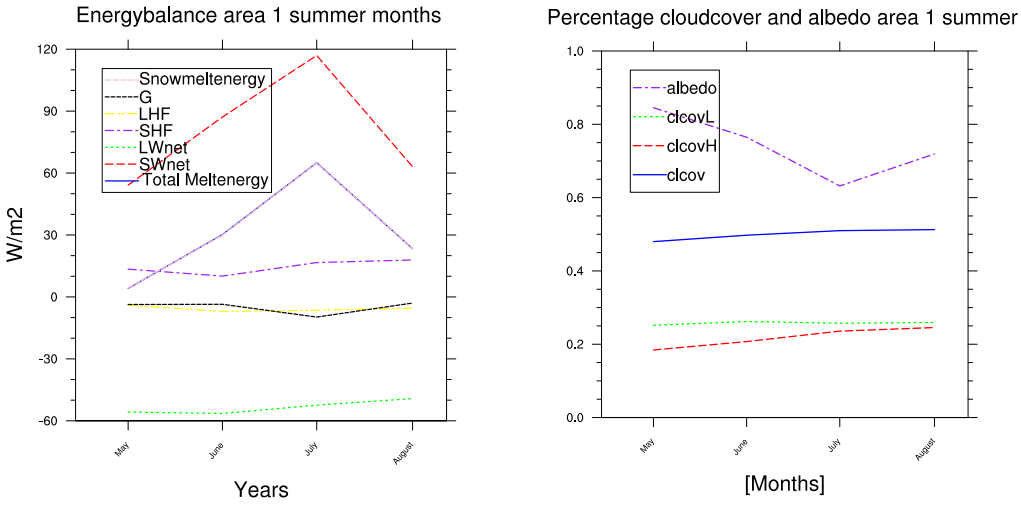


Figure 13: Figure (a) and (b) show respectively the energy balance components and different parameters, for the summer months averaged over 56 years since 1958. clcocL: Low cloud cover, clcov:cloud cover, clcovH: High cloud cover

Figure 14 shows that the snowalbedo has a very high negative linear correlation with the snowmelt ($R = -0.95$). This is also observed in the other three regions (not shown). For these regions the correlation R between total melt and the surface albedo is 0.90, 0.86 and 0.75, respectively. This clear relation between melt and albedo is known as the melt-albedo feedback. Ice is darker than fresh snow and has a lower albedo. Regions with ice at the surface will reflect less $SW_{down}$ back than regions with fresh snow at the surface. Therefore, the $SW_{net}$ will be larger at regions with ice at the surface and there will be more energy available for melt. Due to increase in melt, more ice will come to the surface, which results again in a lower albedo.

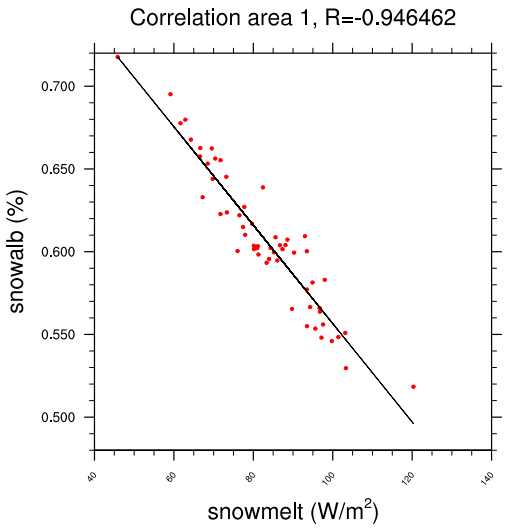


Figure 14: Correlation in July between total melt (snowmelt) and the snowalbedo in area 1.

### 3.2.1 Correlations

Possible links between the changes in the $SEB$ components and the change in melt for the GrIS can be found by looking at the correlations between them for the 56 years since 1958. Table 1 shows all the $SEB$ components correlated with the total melt energy in July for all four areas since 1958. Table 2 shows the linear regression between the energy balance components and the total melt.

Tables 1 and 2 show that in area 1 the $SW_{net}$ has got the highest correlation with the total melt energy ($M$) with $R = 0.87$ and the highest regression of 0.87. The $SHF$ correlates with $M$ with $R = 0.86$, but has a much lower regression of 0.24. The $GHF$ correlates with $M$ with $R = -0.82$ and has also a low regression of -0.18. The $LHF$ correlates with $M$ with $R = 0.49$, but has a very small regression of 0.07. The other $SEB$ components have very weak correlations and very low regressions with $M$. Due to its high correlation and the highest regression of all the $SEB$ components, the increase in $SW_{net}$ is driving the increase in melt in area 1. The $SHF$ is here the second largest $SEB$ component which drives the increase in melt. The $GHF$ has here a negative correlation and has the third largest regression. This regression is negative and the $SHF$ works therefore as an opposing force on the increase in melt.

In area 2 has the $SHF$ got the highest positive correlation with M with $R = 0.70$ and a regression of 0.25. The $SW_{net}$ has here a correlation coefficient $R = 0.68$ and a regression of 0.74. The $GHF$ has a negative correlation with $R = -0.74$ and a regression of 0.25. The $LHF$ has a correlation of $R = 0.58$ and has a slope of 0.14. The other $SEB$ components have again a very weak correlations and very low regressions with $M$. In this area again the $SW_{net}$ is the $SEB$ component that primarily drives the increase. The $SHF$ and $LHF$ are also driving components. The $GHF$ is again negative correlated with total melt.

In area 3 the $SW_{net}$ has the highest correlation with $R = 0.71$ and highest regression of 0.86. The $GHF$ has the second largest positive correlation with $R = 0.67$ and a regression of 0.18. The $LW_{down}$ has a correlation of $R = 0.48$ and a regression of 0.85.

In area 4 the $GHF$ and $LW_{down}$ have the highest positive correlations, and also high regressions. This implies that the increasing $GHF$ and $LW_{down}$ are the drivers for the increase in melt. The correlations of the $LHF$ and $SHF$ with the melt energy are negative. These $SEB$ components are decreasing in this area.

Comparing the correlations of the $SEB$ components with the total melt energy for the four areas since 1958, we can see that there are some links and some remarkable differences. For instance the $SW_{net}$ is an important driver of melt in area 1, but becomes less important if we go down to area 4. Since the $SW_{down}$ hasn't changed over the whole GrIS in the 56 years since 1958 (Figure 15), this change in $SW_{net}$ will probably be due to the relative high decrease in albedo in area 1 compared with the lower decrease in albedo in area 4. The regression and correlation of the $LW_{down}$ with the melt are in areas 1 and 2 very low, while they are higher in areas 3 and 4. Together with the decrease of correlation of $SW_{net}$ with the melt, it implies that the $LW_{down}$ is a more important driver of melt than the $SW_{net}$ in areas 3 and 4. The $LW_{down}$ is affected by the clouds and the $SW_{net}$ by the sun and albedo. This shows that the melt in the ablation and melt zones (areas 1 and 2) are more effected by the changes in albedo and sun radiation and that the melt in the wet snow zone and dry snow zones (areas 3 and 4) are more effected by cloudy weather conditions. The $GHF$ has a negative correlation with the total melt in areas 1 and 2 and a positive one in areas 3 and 4. This is because the total refreeze is decreasing in areas 1 and 2 and increasing in areas 3 and 4. In area 4 the regression of the $GHF$ is 0.61, this implies that the $GHF$ and therefore also the refreeze play a large role in the melt process in area 4. The $SHF$ is in areas 1 and 2 a relative important driver of melt while this is not the case for areas 3 and 4. This will be investigated in paragraph 3.2.3.

| Correlation with M $[W/m^2]$ | | | | |
|---|---|---|---|---|
| $SEB$ component | Area 1 | Area 2 | Area 3 | Area 4 |
| $SW_{net}$ | 0.87 | 0.68 | 0.71 | 0.36 |
| $SW_{down}$ | 0.04 | 0.14 | -0.29 | -0.37 |
| $LW_{net}$ | 0.02 | 0.07 | -0.06 | 0.08 |
| $LW_{down}$ | 0.23 | 0.14 | 0.48 | 0.48 |
| $LHF(latf)$ | 0.49 | 0.58 | -0.22 | -0.75 |
| $SHF(senf)$ | 0.86 | 0.70 | 0.15 | -0.42 |
| $GHF(gbot)$ | -0.82 | -0.74 | 0.67 | 0.87 |

Table 1: Correlation coefficient per area of all the components of the $SEB$ in $[W/m^2]$ with M (the total melt energy) $[W/m^2]$

| Regression | | | | |
|---|---|---|---|---|
| $SEB$ component | Area 1 | Area 2 | Area 3 | Area 4 |
| $SW_{net}$ | 0.87 | 0.74 | 0.86 | 1.19 |
| $SW_{down}$ | 0.03 | 0.22 | -0.52 | -3.04 |
| $LW_{net}$ | 0.01 | 0.05 | -0.06 | 0.38 |
| $LW_{down}$ | 0.09 | 0.12 | 0.85 | 4.6 |
| $LHF(latf)$ | 0.07 | 0.14 | -0.03 | -0.72 |
| $SHF(senf)$ | 0.24 | 0.25 | 0.04 | -0.57 |
| $GHF(gbot)$ | -0.18 | -0.17 | 0.18 | 0.61 |

Table 2: Regressions per area between the components of the $SEB$ $[W/m^2]$ and M (total melt energy) $[W/m^2]$

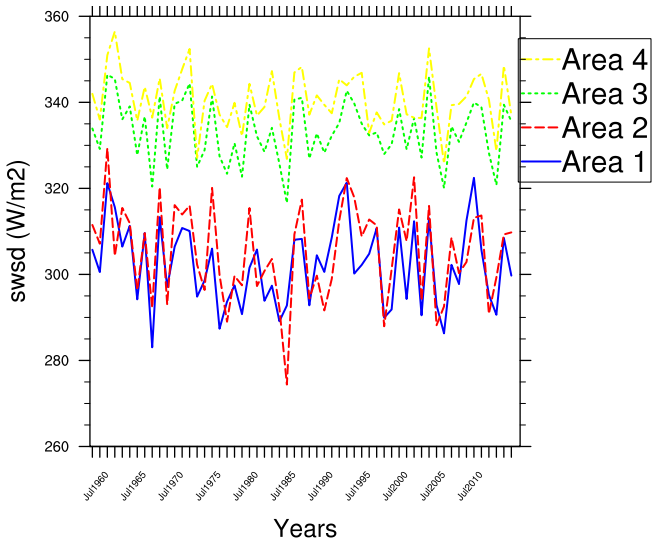


Figure 15: Timeseries of the $SW_{down}$ in July

### 3.2.2 Energy diagram

In order to understand the correlations between the $SEB$ and melt, the daily weather and $SEB$ is analysed for grid points in all four areas and for a warm and cold year. Figure 16 shows the data for a location in area 2 for a warm year (2012). Two different types of melting conditions are visible. The first type is melt during sunny weather, which occurs most often at this location. During this weather type, $SW_{down}$ is high (300-400 W/m$^2$) but only about 30% is absorbed because a snow layer is still present at the surface. $LW_{down}$ is about 200 W/m$^2$ and as a result $LW_{net}$ is negative. Since temperatures are above $0°C$, $SHF$ and $LHF$ are positive. However, wind speeds are relatively low so these turbulent fluxes are not large. As a result, during these sunny days about 60-80 W/m$^2$ is available for melting. Finally, $GHF$ in this area is positive for most days in July, indicating that during these nights, when indeed the surface temperatures drop below $0°C$, refreezing occurs.

The second type of melting days are windy and cloudy days. Due to the clouds $SW_{down}$ and $SW_{net}$ are reduced, but $LW_{net}$ is about 0 W/m$^2$ as the low clouds are as warm as the surface. For the cloudy and windy days, enhanced mixing ramps up the turbulent fluxes, providing ample energy for melting. Hence, for these cloudy days, the energy available for melting can reach for this specific month and site to up to 160 W/m$^2$. If we compare this behaviour of melt in relation to the actual weather for area 1 (not shown), it stands out that for the sunny days, the available energy for melt in area 1 is much higher due to the lower albedo. In July, the snow has disappeared for the majority of gridpoints in area 1. As the impact of $SW_{down}$ on the melt rate is much stronger in area 1 than in area 2, cloudy days in area 1 don't necessarily have higher melt rates than sunny days. Still, melt energy can peak during these windy and cloudy days. Concluding, the different surface albedo causes the difference in dependency on $SW_{net}$ between area 1 and area 2. The daily weather and $SEB$ for gridpoints in areas 3 and 4 (not shown), show even lower $SW_{net}$, due to a higher surface albedo. The peaks in $SHF$ and $LHF$ at windy and cloudy days are less high in areas 3 and 4 than in areas 1 and 2 but are together with the $LW_{down}$ responsible for most of the melt in these areas. In area 1 the minimum and maximum temperatures in July are very often above $0°C$, which means few nights with refreezing. Therefore the $GHF$ in area 1 is in July. The data of the arbitrary gridpoint in area 3 (not shown), shows that there are many nights in this area with temperatures below $0°C$ and that this gives here a larger $GHF$ than areas 1 and 2. Due to these colder temperatures in areas 3 and 4, there is less melt than in areas 1 and 2.

During a refreezing process of water in the firnlayer there is heat emitted. Ice cold itself is cold and the water on the icelayer undergoes not much refreezing, so there is approximately no heat emitted. As earlier analyzed, areas 1 and 2 have higher minimum temperatures than areas 3 and 4. Due to the increasing minimum temperatures at night in the 56 years since 1958, the temperatures in area 1 and 2 are more regular above $0°C$ and without any refreezing. Areas 3 and 4 have most of the nights temperatures below $0°C$. With the increasing temperatures these areas will have more days with melt and nights with refreezing. An increase in refreeze means automatically an increase of the $GHF$. This is the reason why the $GHF$ has a negative correlation in areas 1 and 2 and a positive correlation in areas 3 and 4. The figure also shows that after days with melt and high temperatures at places with a firnlayer, there will be heat in the firnlayer. The emitting of this heat causes an increase in $GHF$.

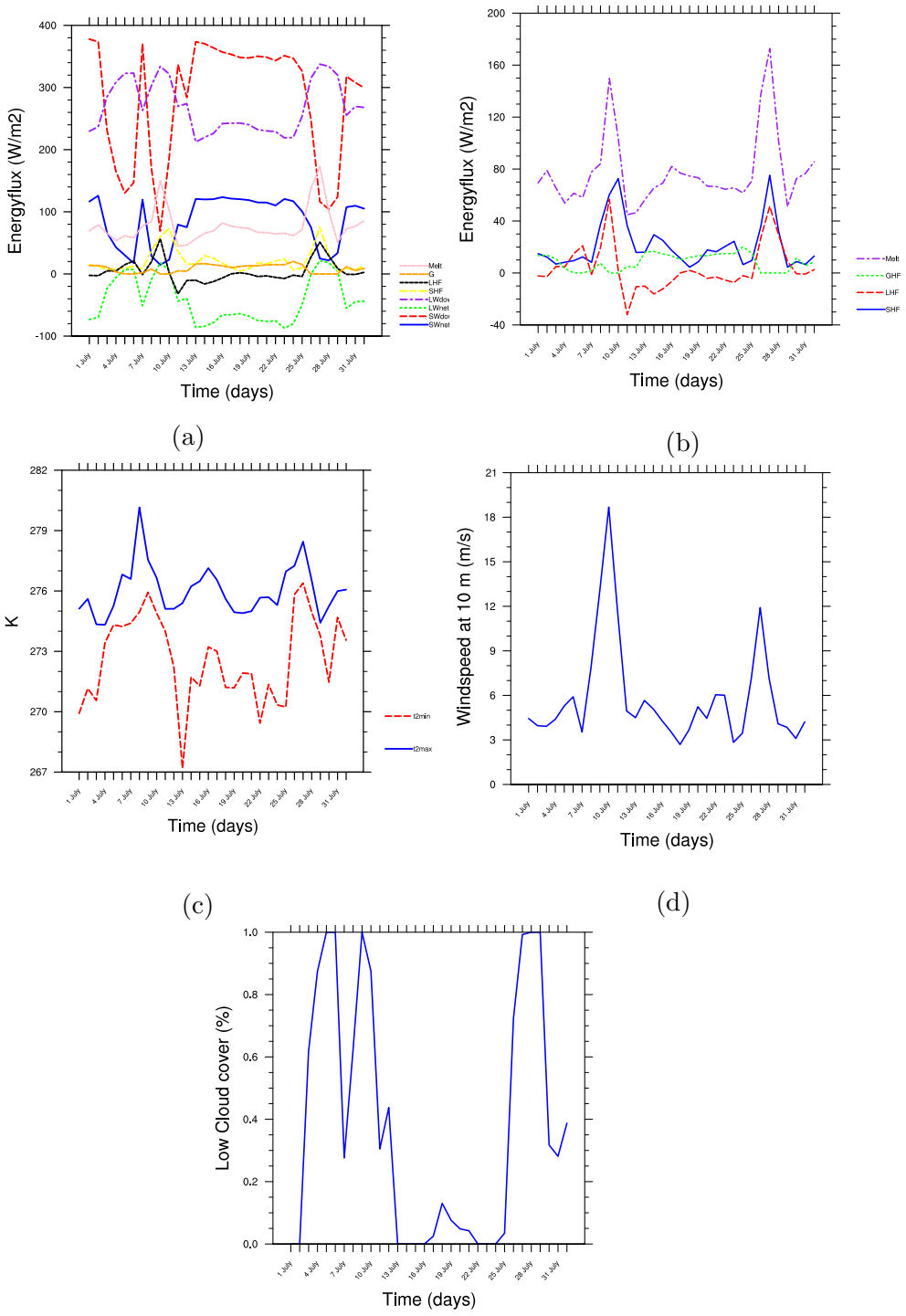


Figure 16: The climate of a grid box in area 2, at 61.5 °N, 46.84 °W, for July 2012; a) the surface energy balance components; b) melt energy, turbulent fluxes and ground heat flux; c) Minimum and maximum daily temperature at 2m elevation d) daily mean wind speed at 10 m and e) low cloud cover.

### 3.2.3 Factors controlling the SHF

Table 1 shows that the $SHF$ has a good correlation with the melt. Negative correlations in areas 1 and 2 and positive correlations in areas 3 and 4. In this section the change in the $SHF$ is analyzed. Firstly the relation between $SHF$ and windspeed at 10m (ff10m) is analyzed. Table 3 shows for all four areas, the correlation between the windspeed at 10m and the $SHF$, derived for July. These correlations of the $SHF$ with the windspeed at 10 meter elevation indicate that the increase of windspeed is a possible cause of the positive trend of the $SHF$. The windspeed at 10m (ff10m) has increased in area's 1 and 2 and has decreased in area's 3 and 4 over last 57 years (Figure 17a). Due to this increase in windspeed in areas 1 and 2, there will be an increase in turbulence here. Therefore the turbulent fluxes will increase. The $SHF$ and ff10m correlate in area 1 with $R = 0.68$ and in area 2 with $R = 0.77$ (Tables 3 and 4). The correlations and regressions do not describe the decrease of the $SHF$ in areas 3 and 4. Secondly, the relation between the low cloudcover and the $SHF$ has been analyzed. Figure 16 shows that a high $SHF$ occurs often at days with a high degree of low cloud cover, which suggests a possible link. Figure 17b shows that the low cloud cover decreases in all areas. This decrease in low cloud cover contradicts with the theory, that the increase in low cloud cover is a drive of the increase in $SHF$. The factors windpeed at 10m and low cloudcover only, are not enough to explain the trend of the $SHF$ in areas 3 and 4. Therefore we look to the increase in temperature at 2 meter elevation. Table 4 shows that the temperature at 2m and the $SHF$ have good positive correlations with each other in areas 1 and 2 and have negative correlations in areas 3 and 4. If the 2m temperature increases, the downward temperature gradient will become smaller. In the summer, the temperature of the surface ice and firn in areas 1 and 2 is often around 0 $°C$, due to the heating released by melt. These surface temperatures will rise less quickly than the relative cold firn layers of areas 3 and 4. Therefore the surface temperatures in areas 3 and 4 will have a higher rate of increase. This increase in temperature at the surface in areas 3 and 4, causes the temperature gradient to become smaller and have therefore a reducing effect on the $SHF$.
The difference between the increase per decade in temperatures at 2m elevation and the temperatures at 5500m elevation in area 3 in July over the last 57 years has become around $0.044K/decade$ (Table 5). In area4 around $0.023K/decade$. The correlation between the temperature gradient and the $SHF$ is in area 3 $R = -0.08$ and in area 4 $R = -0.15$. These are very weak correlations. Even though the temperature gradient is known to be a driver of the $SHF$, these correlations are not good enough to directly link them in these areas.

| Correlation with $SHF$ in $[W/m^2]$ | | | | |
|---|---|---|---|---|
| | Area 1 | Area 2 | Area 3 | Area 4 |
| clcovl | -0.40 | -0.28 | -0.65 | -0.75 |
| ff10m (m/s) | 0.68 | 0.77 | 0.39 | 0.37 |
| t2m (K) | 0.78 | 0.62 | -0.09 | -0.51 |
| t0500-t2max (K) | -0.49 | -0.27 | -0.08 | -0.15 |

Table 3: Correlation coefficient per area of different parameters from 1958 till 2014

| Regression | | | | |
|---|---|---|---|---|
| | Area 1 | Area 2 | Area 3 | Area 4 |
| clcovl | -0.0060 | -0.0066 | -0.0328 | -0.0364 |
| ff10m(m/s) | 0.0499 | 0.0833 | 0.1298 | 0.1325 |
| t2m (K) | 0.1085 | 0.1286 | -0.0873 | -0.5755 |
| t0500-t2max (K) | -0.1037 | -0.0847 | -0.0407 | -0.0872 |

Table 4: Regression per area of the different parameters with the $SHF$ in $[W/m^2]$ from 1958 till 2014

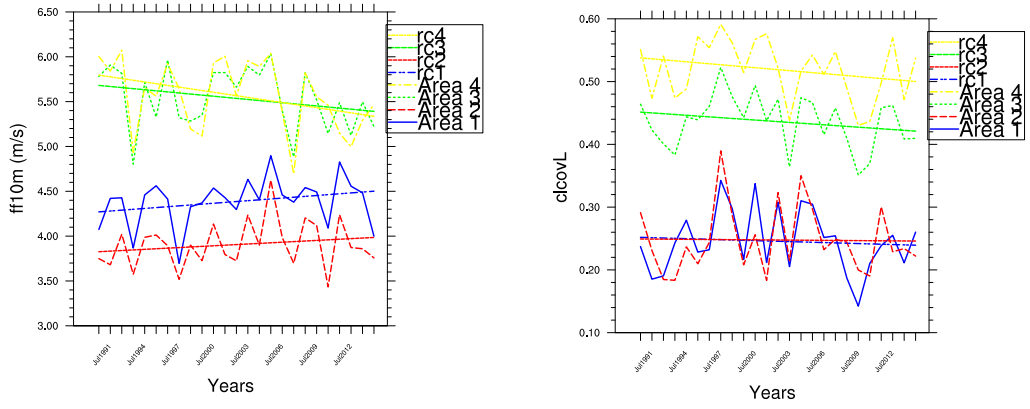


(a) (b)

Figure 17: 10m Windspeed (a) and low cloud cover (b) per area in July since 1990

| Delta T (K/decade) | | | | |
|---|---|---|---|---|
| | Area 1 | Area 2 | Area 3 | Area 4 |
| t2max | 0.117 | 0.124 | 0.196 | 0.252 |
| t0500 | 0.239 | 0.198 | 0.240 | 0.275 |
| t0500-t2max | 0.122 | 0.074 | 0.044 | 0.023 |

Table 5: This table shows the increase per decade for: the maximum temperature at 2 meter elevation (t2max), the temperature at a elevation at which the pressure is $500hPa$ and the difference t0500-t2max, from 1958 till 2014

# 4 Discussion

## 4.1 Model limitations

During the research we found that the model works differently than initially expected. RACMO2.3 calculates that when it rains, there will also be a minority of snowfall, which forms a thin layer of snow water mixture on the surface. In cases of a thin layer of snow water mixture RACMO2.3 assumes, that there will be only firn runoff and no ice runoff. This implies that only when there is no rain, there can be ice runoff. This way of calculation of RACMO2.3 may be incorrect and leads in this research to an undesired partitioning between firn runoff and ice runoff. Therefore we have adapted the model data and assumed that up to a layer of 3 cm snow on top of the ice sheet only ice runoff can occur. We defined that there can be a 3 cm firnlayer if the total pore space at that point is less than 2 cm. The use of this 3cm firnlayer for the partitioning of the ice and firn areas is not yet justified by any research.
The usage of the four areas gives more insight in the similarities and differences between melt processes in different regions and is therefore very useful. The results achieved by using the four areas, depend to a large extend on how good RACMO2.3 models the firnlayer and whether our adaption of the model data is correct. These similarities and differences found by using the four areas, could not have been seen if we only investigated the integrated values of the $SWB$, $SMB$ and $SEB$. For defining the ice and firn runoff more accurately, more research on the 3 cm firnlayer is recommended. Before trying this adaption, we looked at the surface snow density as a possible indicator for ice and firn melt. Since this gave a same wrong result, we abandoned this method.
Even though the data generated from the model largely agrees with the observational data, there are still some parameters that differ from it. In order to get even more preciser results in the future it is necessary to improve the model and to reduce the gridsize. Smaller gridsizes will make it possible to study local variability's better.
Only the summer months were used for studying the parameters, especially the month July. Even though the melt and runoff are very low in the other months, they can still be of some significance, since the melting season is shifting and begins earlier. It is therefore wise to take these months before and after the summer also into account in future research.

## 4.2 Future research

The $SHF$ is defined to be dependent on the windspeed and temperature gradient. The temperature gradient appeared to correlate very weak. These odd and unexpected correlations could be further studied in the future. We did not investigate the change in sublimation due to it's relative small contribution to the $SMB$. This change in sublimation could be a subject too for further investigation.

# 5 Conclusions

The data of the last 57 years shows a clear difference between all $SWB$ components in the four different areas. The ice runoff is in area 1 the largest sink of the $SWB$. The increase in ice runoff is here approximately equal to the increase in ice melt. The firn runoff and ice and firn refreeze have decreased here. The firn runoff in this area is primarily driven by the melt of the snowfall from the winter. In area 2 is the firn runoff the largest sink of the $SWB$. The increase in firn runoff here is caused by a slight increase in firn melt and a decrease in refreeze of firn melt. The ice runoff and ice melt are lower than the firn runoff and firn melt, but show an increase in this area. In area 3 is the refreeze of firn melt the largest sink of the $SEB$. The melt in this area is primarily firn melt. The firn runoff increases in this area, but is much lower than the firn melt. This is due to the large firn refreeze component. Here, the ice runoff is lower than the firn runoff, but shows an increase. Area 4 experiences almost only melt of firn and refreeze of firn. Therefore, the firn runoff is here very small. Even though the ice and firn runoff are very small, they still show an icrease. It is remarkable that the ice runoff increases in all four areas. The firn runoff only increases in areas 2,3 and 4 and decreases in area 1. The refreezing only increases in areas 3 and 4 and decreases in areas 1 and 2. The data shows that the total ice runoff has increased more than the total firn runoff in the last 57 years and has a higher contribution to the reduction of $SMB$ than the firn runoff. Since the ice runoff is primarily ice-melt, and the firn runoff firn melt, we can conclude that the ice-melt is the biggest contributor to the increase in ice runoff and therefore the biggest contributor to the reduction of the $SMB$. The decrease of refreeze in areas 1 and 2 in July imply that the melting season is shifting and is starting earlier in the summer.

The increase in total melt is for a large part driven by changes in the $SEB$ components. The contribution of the $SEB$ components to this increase in melt energy varies for the four areas. The increase in melt in areas 1 and 2 is primarily driven by the increase in $SW_{net}$. The increase in $SW_{net}$ is largely caused by the decrease in the surface albedo. This decrease in surface albedo is strongest in area 1 and the weakest in area 4. Other drivers of the increase melt in areas 1 and 2 are the $SHF$ and $LHF$, while the $GHF$ is decreasing.
The regression and correlation of the $LW_{down}$ with the melt are in areas 1 and 2 very low, while they are higher in areas 3 and 4. Together with the decrease of correlation of $SW_{net}$ with the melt, it implies that the $LW_{down}$ is an important driver of the melt in areas 3 and 4. The $LW_{down}$ is affected by the degree of clouds in the atmosphere. In areas 3 and 4 is the $GHF$ a driver of melt. The $SHF$ and $LHF$ are decreasing and therefore lowering the increase in melt.

The decrease in the $GHF$ in areas 1 and 2 is driven by the decrease in refreeze in these areas, caused by increasing minimum temperatures at night in the 56 years since 1958. Areas 3 and 4 have lower minimum temperatures than areas 1 and 2. These minimum temperatures have increased and cause an increase in refreezing. The $GHF$ shows therefore in areas 3 and 4 also an increase. The increase in $SHF$

has a good correlation with the increase in windspeed at 10m elevation in areas 1 and 2 and has therefore also a good correlation with an increase in turbulence in the air in these areas. We can thus conclude that the increase in windspeed at 10m elevation is a driver of the increase in the $SHF$ and the $LHF$ in these areas. The analysis of the $SHF$ also showed that the decrease in $SHF$ and $LHF$ in areas 3 and 4 is caused by the increase in temperature at 2m elevation. This increase causes a decrease in the the temperature gradient and has therefore a reducing effect on the $SHF$ and $LHF$.

# 6 Acknowledgements

I want to thank my supervisor dr. Willem Jan van de Berg for his guidance and support during this research. I also want to thank Stan Jakobs for helping me getting familiar with NCL in the beginning of my research.

# References


[1] Andrew Shepherd et al. A reconciled estimate of ice-sheet mass balance. *Science*, 388:1183–1189, 2012.

[2] Edward Hanna et al. Ice-sheet mass balance and climate change. *Nature*, 498:51–59, 2013.

[3] Peter Lemke et al. *Climate change 2007: The physical science basis.* Cambridge University Press, 2007.

[4] W.J. van de Berg F. C. Bosveld B.J.J.M. van den Hurk G. Lenderink E. van Meijgaard, L.H. van Ulft and A.P. Siebesma. *The KNMI regional atmospheric climate model RACMO version 2.1.* Techincal report 302. KNMI, 2008.

[5] Janneke Ettema. *The present-day climate of Greenland A study with a regional climate model.* Ph.D. thesis. Utrecht University, 2010.

[6] Ruth H Mottram. The surface mass balance of the greenland ice sheet, http://polarportal.dk.

[7] Michiel van den Broeke. *The atmospheric boundary layer over ice sheets and glaciers.* Ph.D. thesis. Utrecht University, 1996.